NOAA Technical Memorandum ERL NSSL–94

MULTIPLE DOPPLER RADAR DERIVED VERTICAL VELOCITIES IN THUNDERSTORMS
PART I – ERROR ANALYSIS AND SOLUTION TECHNIQUES
PART II – MAXIMIZING AREAL EXTENT OF VERTICAL VELOCITIES

Stephan P. Nelson
Rodger A. Brown

National Severe Storms Laboratory
Norman, Oklahoma
October 1982

noaa NATIONAL OCEANIC AND ATMOSPHERIC ADMINISTRATION / Environmental Research Laboratories

NATIONAL OCEANIC AND ATMOSPHERIC ADMINISTRATION

ENVIRONMENTAL RESEARCH LABORATORIES

NATIONAL SEVERE STORMS LABORATORY TECHNICAL MEMORANDA

The National Severe Storms Laboratory, Norman, Oklahoma, in cooperation with other government groups and with units of commerce and education, seeks understanding of tornadoes, squall lines, thunderstorms, and related local storms and rain; develops and applies methods for their observation and prediction; and examines possibilities for their beneficial modification.

Reports by the cooperating groups are printed as NSSL Technical Memoranda, a subseries of the NOAA Technical Memorandum series, to facilitate prompt communication of information to vitally interested parties and to elicit their constructive comments. These Memoranda are not formal scientific publications.

The NSSL Technical Memoranda, beginning with No. 28, continue the sequence established by the U.S. Weather Bureau National Severe Storms Project, Kansas City, Missouri. Numbers 1-22 were designated NSSP Reports. Numbers 23-27 were NSSL Reports, and 24-27 appeared as a subseries of Weather Bureau Technical Notes.

Reports in this series are available from the National Technical Information Service, Operations Division, Springfield, Virginia 22151.

NOAA Technical Memorandum ERL NSSL-94

MULTIPLE DOPPLER RADAR DERIVED VERTICAL VELOCITIES IN THUNDERSTORMS

PART I - ERROR ANALYSIS AND SOLUTION TECHNIQUES

Stephan P. Nelson
Rodger A. Brown

PART II - MAXIMIZING AREAL EXTENT OF VERTICAL VELOCITIES

Rodger A. Brown
Stephan P. Nelson

National Severe Storms Laboratory
Norman, Oklahoma
October 1982

UNITED STATES
DEPARTMENT OF COMMERCE
Malcolm Baldrige,
Secretary

NATIONAL OCEANIC AND
ATMOSPHERIC ADMINISTRATION
John V. Byrne,
Administrator

Environmental Research
Laboratories
George H. Ludwig
Director

TABLE OF CONTENTS

TABLE OF CONTENTS

LIST OF FIGURES

PART I

PART II

List of Figures Cont'd

LIST OF SYMBOLS

b	Denotes a quantity at either the top or bottom boundary of the Doppler data
b'	Denotes a quantity at the opposite boundary of "b".
n	Denotes a quantity at the "n^{th}" height level (relative to lower boundary).
s	Subscript used to denote quantities at "ground" level as defined by grid construction.
t	Denotes a quantity at the top data level with respect to the ground.
u	West-east component of air velocity
v	South-north component of air velocity.
V_t	Mean terminal fall velocity of precipitation in clear air.
w^c	Vertical velocity computed from multiple-Doppler analysis.
w	Vertical component of air velocity.
Δw_b	Difference between computed vertical velocity at level b and the assumed boundary value ($\Delta w_b = w_b^c - w_b$).
z	Vertical Cartesian distance.
$\lvert\Delta z\rvert$	Absolute value of vertical grid spacing.
$\nabla_h \cdot \vec{v}$	Horizontal divergence.
β	Boundary error in vertical velocity.
δ	Index. $\delta=1$ for upward integration and $\delta=-1$ downward integration.
ε	Error in multiple-Doppler computed horizontal divergence.
ρ	Air density.

MULTIPLE DOPPLER RADAR DERIVED VERTICAL VELOCITIES IN THUNDERSTORMS: PART I - ERROR ANALYSIS AND SOLUTION TECHNIQUES

Stephan P. Nelson and Rodger A. Brown

Abstract

A detailed error analysis is performed on the problems associated with using multiple Doppler radar data and the continuity equation to solve for the vertical component of motion in deep convective storms. The errors considered are those due to either incorrect boundary values or errors encountered in integrating the horizontal divergence with height.

Data show that errors in the integrated horizontal divergence are much larger than previously thought--indicating the previously ignored effects of bias values may be an important error source. A simple vertical velocity adjustment technique is presented which yields fairly accurate results under most conditions. In the unusual case, though, of reinforcing bias errors (e.g., excessive convergence in low levels capped by excessive divergence) the unadjusted profile obtained by downward integration yields better results at most levels than the adjusted profile.

The effects of boundary errors on both adjusted and unadjusted vertical velocity profiles also are examined in detail.

1. INTRODUCTION

The benefits of Doppler radar to the meteorological community are well known. Retrieval of three dimensional wind fields from synthesis of two or more Doppler radars contributes significantly to the understanding of kinematics, dynamics, and even thermodynamics (Gal-Chen, 1978; Hane and Scott, 1978) of various meteorological systems. In general, early studies limited quantitative discussions of vertical velocities to the lowest few kilometers (e.g., Brown and Peace, 1968; Lhermitte, 1970; Brown et al., 1975; Brandes, 1977; Burgess et al., 1977; Heymsfield, 1978). This lower level limitation was usually due to unrealistic vertical velocities that were obtained after a few upward integration steps of the continuity equation (Ray and Wagner, 1976; Burgess et al., 1977; Kelly et al., 1978). Large errors in vertical velocity are not consistent with the theoretical calculations of Bohne and Srivastava (1975), Doviak et al. (1976), and Ray et al. (1980). Assuming only random errors in measured Doppler velocities, these authors found that vertical velocities may be calculated with an error variance of 10 $m^2 s^{-2}$. Using actual data it is shown that vertical velocity errors are an order of magnitude larger than predicted by this theory.

In this study we investigate the nature of both boundary and nonrandom horizontal divergence errors using actual data and model profiles. This analysis includes the effects of these errors on both constrained and unconstrained vertical velocity profiles. Brown and Nelson (1982) discuss problems associated with applying the results of this work to actual data.

2. BASIC EQUATIONS

The simplified form of the continuity equation is given by

$$w_n = w_b \frac{\rho_b}{\rho_n} - \frac{1}{\rho_n} \int_{z_b}^{z_n} \left[\rho (\nabla_h \cdot \vec{v}) \, dz \right] \tag{1}$$

where these and all other symbols are defined in the List of Symbols. The u and v components required for the horizontal divergence are calculated via the dual or three or more Doppler equations (e.g., Armijo, 1969). For this paper attention is limited only to the errors involved in solving Eq. (1) given erroneous boundary values and nonperfect measurements of horizontal divergence. The density terms and numerical approximations are assumed to be exact. Using the trapezoidal integration approximation, Eq. (1) becomes:

$$w_n = w_b \frac{\rho_b}{\rho_n} - \frac{\delta}{\rho_n} \frac{|\Delta z|}{2} \sum_{i=b}^{n-\delta} \left[\rho_i (\nabla_h \cdot \vec{v})_i + \rho_{i+\delta} (\nabla_h \cdot \vec{v})_{i+\delta} \right] \tag{2}$$

where the vertical grid system is indicated in Fig. 1, for upward integration, b=1, δ=+1; for downward integration b=t, δ=-1. If β is the error associated with estimation of the boundary vertical velocity and ε the error in computed horizontal divergence, then

$$w_n^c = w_n + \beta_b \frac{\rho_b}{\rho_n} - \frac{\delta}{\rho_n} \frac{|\Delta z|}{2} \sum_{i=b}^{n-\delta} \left[\rho_i \varepsilon_i + \rho_{i+\delta} \, \varepsilon_{i+\delta} \right] \tag{3}$$

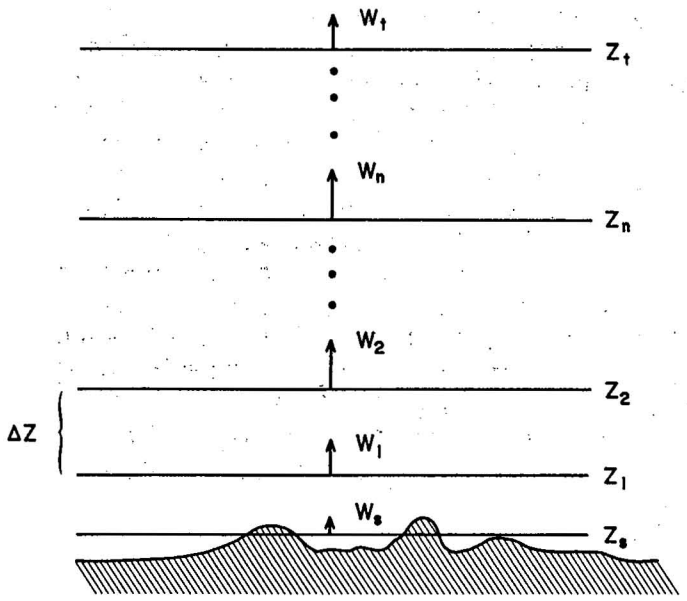

Figure 1. Vertical grid system used in computing vertical velocities. Plane z_s is positioned at a height roughly equal to the mean ground level. Lowest and highest data are at levels z_1 and z_t, respectively.

where w_n^c is the computed vertical velocity at any level "n". Since it is the analyst's task to retrieve w_n from w_n^c by either minimizing or correcting for the error terms, it is necessary to take a close look at the sources and nature of these errors.

3. BOUNDARY CONDITION ERRORS - β

For upward integration the error in vertical velocity at any level "n" due to a boundary error is

$$\beta_1 \frac{\rho_1}{\rho_n} \tag{4}$$

Because of radar beam propagation relative to the curved earth's surface, the lowest data level (z_1, Fig. 1) is usually a few hundred meters above the "ground" (z_s, Fig. 1). Additionally, the "ground" level is typically established by the analyst as some intermediate level between the highest and lowest terrain features. The boundary vertical velocity (w_1) is obtained by assuming a divergence value at z_s and integrating to z_1 using the boundary value w_s=0. Non-zero values of w_s can arise in two ways. First of all, nonuniform terrain can cause an "upslope" vertical velocity at z_s. For example, in central Oklahoma a large elevation change would be 300 m in altitude over 10 km in horizontal range. Assuming a 10 m s^{-1} horizontal wind, this gives rise to a vertical velocity of less than 0.5 m s^{-1}. Vertical velocities at z_s can also appear because of convergence below the plane z_s. Strong surface convergence can be of the order 10^{-2} s^{-1}. If this operates over a 100 m depth below z_s the boundary vertical velocity is then about 1 m s^{-1}. These two factors give a combined maximum error in w_s of less than 2 m s^{-1}.

The second problem arises in estimating the divergence at z_s. Errors in this estimate may be of the order 10^{-3} s^{-1}. With a 500 m spacing between z_s and z_1, this results in a 0.25 m s^{-1} error in w_1. Overall the errors in w_1 should be less than 2 m s^{-1}. Any errors, of course, are amplified by the ratio ρ_1/ρ_n. The ratio of standard atmospheric densities versus height for upward integration is shown as the dashed line in Fig. 2 (see also Bohne and Srivastava, 1975). For example, a 2 m s^{-1} error at the surface grows to about 11 m s^{-1} at 15 km.

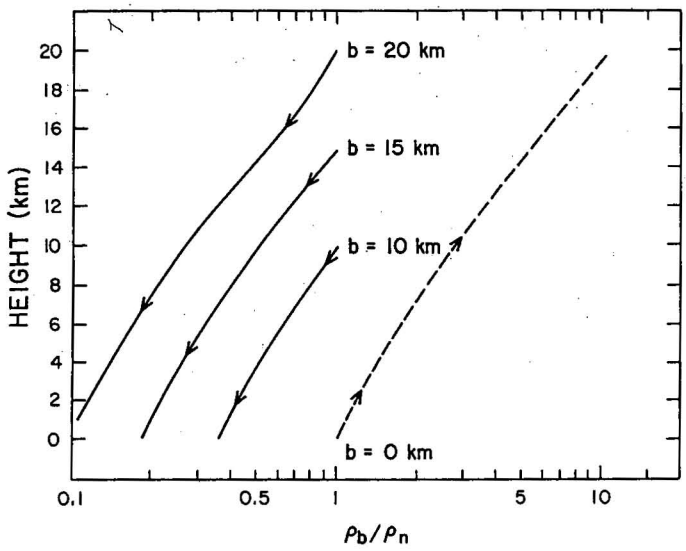

Figure 2. Ratio of air density of top and bottom boundaries (ρ_b) to air density at height "n" (ρ_n). Dashed line corresponds to upward integration (ρ_b at 0.0 km). The three solid lines correspond to downward integration (ρ_b at 10, 15, and 20 km).

Integrating downward, the boundary error is

$$\beta_t \frac{\rho_t}{\rho_n} \tag{5}$$

In this case the density ratios are less than one, as shown in Fig. 2. For the same boundary inaccuracies, therefore, downward integration results in smaller errors than upward integration. Usually, though, the bottom boundary is more accurately known than the top. (Methods of estimating β_t are given in Bohne and Srivastava, 1975; and in Brown and Nelson, 1982). This situation presents the analyst with the problem of using a well known (bottom) boundary condition whose errors amplify, or a lesser known (top) one whose errors are suppressed! An interesting relationship exists between the boundary errors for the two integration directions. Equating the expressions in Eqs. (4) and (5), and rearranging we obtain

$$\beta_t = \beta_1 \frac{\rho_1}{\rho_t} \tag{6}$$

That is, for the vertical velocity errors to be equal at each level irrespective of integration direction, the top boundary condition error must be larger than the bottom boundary condition error by a factor of ρ_1/ρ_t. For example, beginning at 15 km and integrating downward, the top boundary error can be 5.4 times as large as the bottom boundary error and still give the same vertical velocity errors at all levels.

4. DIVERGENCE ERRORS - ε

Using Eq. (3) and ignoring the boundary error term, the computed vertical velocities for upward and downward integration are given by

$$w_n^c = w_n - \frac{\delta}{\rho_n} \frac{|\Delta z|}{2} \sum_{i=b}^{n-\delta} [\rho_i \varepsilon_i + \rho_{i+\delta}\, \varepsilon_{i+\delta}] \tag{7}$$

As with the boundary error, the divergence errors at each level are multiplied by a density ratio greater than one for upward integration and less than one for downward integration. Except for the lowest few kilometers, therefore, downward integration yields the better results as has been emphasized by Bohne and Srivastava (1975) and Ray et al. (1980). In evaluating the error terms, though, these authors

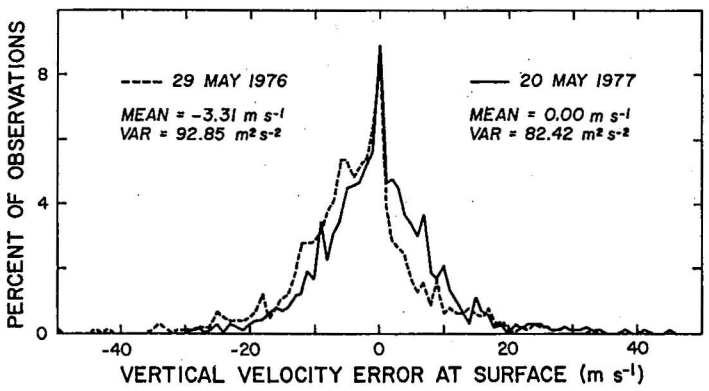

Figure 3. Distribution of computed vertical velocity errors at 1 m s^{-1} intervals. Solid line is from 20 May 1977 dual Doppler synthesis and dashed line is from 29 May 1976 triple Doppler synthesis.

assumed the ε_i's to be random (uncorrelated in the vertical). Using typical uncertainties in Doppler radial velocity estimates, both of these studies computed the expected value of the error term for downward integration to have a mean of zero and a variance of about 10 $m^2\ s^{-2}$. Unfortunately, much larger errors occur with actual data. Fig. 3 shows the distribution from two storms of vertical velocity errors at the surface computed by downward integration. Measurements from the same storm are not independent, but the large variances (~90 $m^2\ s^{-2}$) show that substantial errors are not uncommon. In fact about 40% of these velocity errors lie more than two standard deviations outside the theoretical error range. It is possible that the Doppler velocity estimates are not as accurately known as has been hypothesized; however, it is also possible that the largest errors shown in Fig. 3 arise because of localized nonrandom errors. Effects such as advection/evolution problems (Clark et al., 1980; Carbone, 1981; Gal-Chen, 1981), side lobe contamination, misaligned beams, equipment and meteorological noise are capable of producing such localized bias errors at one or more levels which can then be spread over several grid points by interpolation and any subsequent filtering.

Interesting relationships between computed and actual vertical velocity as a function of ε_i's are apparent from inspection of Eq. (7). If, for example, nonzero ε_i's are all of the same sign, then the profiles from upward and downward integration will bracket the true answer. For illustrative purposes we perturb the "base" divergence profile shown in Fig. 4 by adding a linear error that varies from $-1.0\ 10^{-3}\ s^{-1}$ at 0.0 km to $0.0\ s^{-1}$ at 17 km (curve E_1 on Fig. 4). The results of solving Eq. (2) by both upward and downward integration are shown in Fig. 5. As is expected, except for the lowest few kilometers, downward integration yields

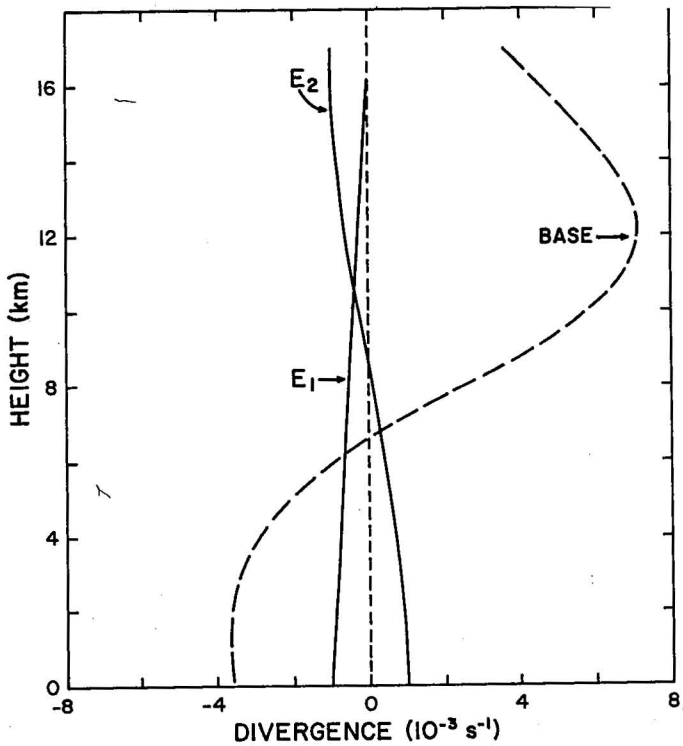

Figure 4. Variation with height of divergence base profile (dashed line) and error curves (E_1, E_2, solid lines). These profiles are used in computing vertical velocities shown in Figs. 5 and 6.

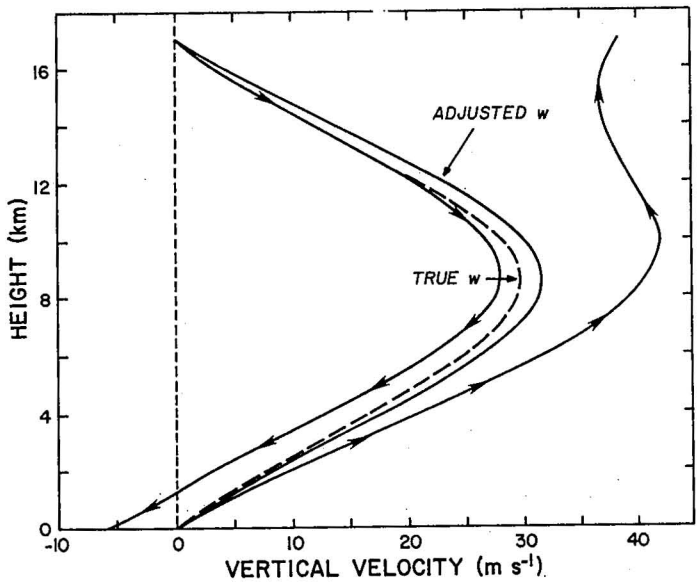

Figure 5. Vertical velocities computed from divergence profiles labeled "base" and E_1 in Fig. 4. The curves computed by upward and downward integration are indicated by solid lines with arrows. The remaining solid curve is the adjusted vertical velocity. The dashed line shows the actual vertical velocity profile.

the better results. Additionally, the upward and downward integration curves form lower and upper bounds to the true answer. This bracketing effect, however, will not necessarily be the case when the ε_i's change sign with height. For example, the errors shown by curve E_2 in Fig. 3, produce the vertical velocity profiles in Fig. 6. Again, in general the downward integration curve is the better of the two, but for most of the vertical depth the upward and downward profiles no longer bracket the true answer.

5. ADJUSTMENTS TO COMPUTED VERTICAL VELOCITIES

Vertical velocities can be adjusted by making certain assumptions. If the errors at each boundary are negligible, then Eq. (3) can be evaluated at the top boundary for upward integration or at the bottom boundary for downward integration

$$w^c_{b'} = w_{b'} - \frac{\delta}{\rho_{b'}} \frac{|\Delta z|}{2} \sum_{i=b}^{b'-\delta} [\rho_i \varepsilon_i + \rho_{i+\delta} \varepsilon_{i+\delta}] \tag{8}$$

where b' is the opposite boundary of b (i.e., if b=1, b'=t, and if b=t, b'=1). All terms in Eq. (8) are known except for the distribution of ε_i. The simplest assumption is that ε is constant with height (Nelson, 1980). Ray et al. (1980) specified ε as a function of the variance of the u,v components due to geometry and radar sampling problems. These values, however, are nearly constant with height, thus these two assumed error distributions basically are equivalent. Eq. (8) therefore can be rearranged

$$\varepsilon = - \frac{\rho_{b'}}{\delta} \frac{2}{|\Delta z|} \frac{\Delta w_{b'}}{\sum_{i=b}^{b'-\delta} [\rho_i + \rho_{i+\delta}]}$$

where $\Delta w_{b'} = w^c_{b'} - w_{b'}$. Substituting this relationship into Eq. (3) (again $\beta_b = 0$, $\varepsilon_i = \varepsilon$ = constant) and rearranging, we obtain

$$w_n = w^c_n - \frac{\rho_{b'}}{\rho_n} \Delta w_{b'} \frac{\sum_{i=b}^{n-\delta} [\rho_i + \rho_{i+\delta}]}{\sum_{i=b}^{b'-\delta} [\rho_i + \rho_{i+\delta}]} \tag{9}$$

which yields an equation to adjust w^c at each level. This equation is similar to the one derived by O'Brien (1970) in the x,y,p coordinate system. Eq. (9) was applied to the vertical velocity profiles shown in Figs. 5 and 6. The ε_i's in these curves were not constant with height; therefore, there is not an exact match between the actual and adjusted curves. In fact, it is interesting to note that in the case of divergence errors changing sign with height (Fig. 6), the adjusted curve is not as accurate as the downward integration curve at most heights!

The above discussion has assumed that both the bottom and top boundaries are accurately known. If errors do exist, then Eq. (9) becomes:

$$w_n = w_n^c - \frac{1}{\rho_n}(\rho_{b'}\,\Delta w_{b'}) \frac{\sum_{i=b}^{n-\delta}(\rho_i+\rho_{i+\delta})}{\sum_{i=b}^{b'-\delta}(\rho_i+\rho_{i+\delta})}$$

$$+ \frac{1}{\rho_n} \frac{\sum_{i=b}^{n-\delta}(\rho_i+\rho_{i+\delta})}{\sum_{i=b}^{b'-\delta}(\rho_i+\rho_{i+\delta})} (\rho_b\beta_b - \rho_{b'}\beta_{b'}) - \frac{1}{\rho_n}\rho_b\beta_b \qquad (10)$$

The adjusted vertical velocity as defined in Eq. (9) will be in error by an amount equal to the last two terms of Eq. (10). This error is plotted in Fig. 7 for $\beta_1 = 1$ m s^{-1} and values of β_t ranging from -10 to +10 m s^{-1}. In this example, errors in the constrained vertical velocity field due to incorrect boundary values should be less than 4 m s^{-1} below 10 km.

6. DISCUSSION

Undoubtedly multi-Doppler radar measurements of updrafts can contribute greatly to the understanding of many meteorological systems. To date little quantitative use has been made of these vertical velocities because of often observed large errors. These errors are typically greater than those predicted by considering only geometry and Doppler sampling problems. The sources of the measurement problems are not known, but side-lobe contamination, misaligned beams, and small scale meteorological noise are possibilities. It would appear reasonable to assume that any such nonrandom errors usually are due to localized problems. It is, therefore, expected that errors in the computed horizontal divergence will be of the same sign and limited to a few levels. In such a case upward and downward integration solutions bracket the actual vertical velocity profile. An exact correction can not be made without

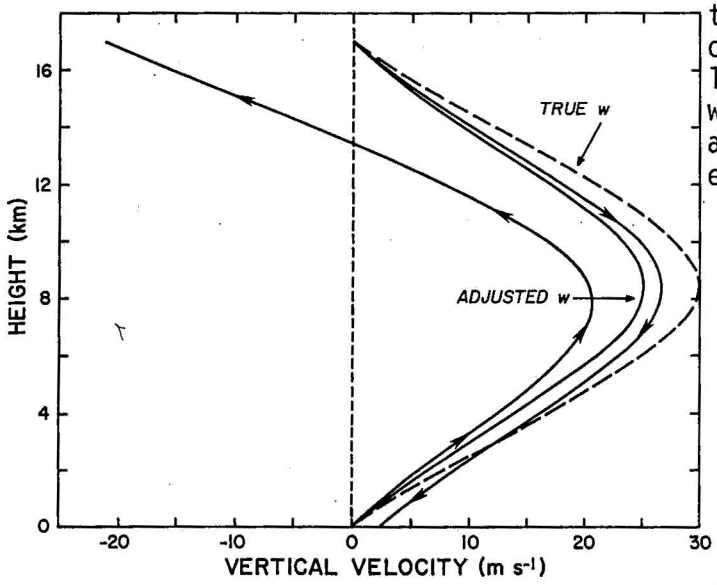

Figure 6. Same as Fig. 5 except for divergence profiles "base" and E_2 given in Fig. 4

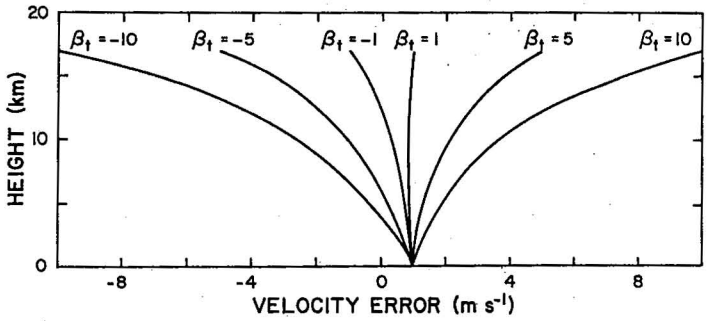

Figure 7. Errors in adjusted vertical velocity profiles due to erroneous lower and upper boundary values. The lower boundary error is 1 m s^{-1}.

knowing the vertical error distribution, but assuming a constant error with height should result in an adjusted curve that is accurate within about 5 m s^{-1} at most levels. This bracketing effect, however, is not the case when there are reinforcing errors at low and high levels (e.g., excessive convergence in low levels and excessive divergence aloft). In this instance, assuming divergence errors are constant with height yields an adjusted curve that is, for most levels, not as accurate as the unadjusted curve obtained by downward integration.

An additional problem in the adjustment process is the effect of erroneous top and bottom boundary values. The magnitude of these errors on the adjusted profile depends on the boundary errors themselves and the depth of integration. The analysis presented here shows such errors should be less than 5 m s^{-1} at levels below 10 km.

In summary if the only problems encountered are random errors in horizontal divergence, then the adjustment technique described here or in Ray et al. (1980) should yield very good results. However, bias errors concentrated at a few levels and incorrect boundary values can degrade the accuracy of the adjusted profile substantially. Errors as large as 10 m s^{-1} may be expected at some levels depending on error magnitudes and locations. In the extreme, if there are reinforcing bias errors in a vertical column, then the adjusted profile may not be as accurate as unadjusted vertical velocities obtained by downward integration at most levels.

Adjustment techniques have reached a fair level of sophistication. At the present time, therefore, the next major advance in computing vertical velocities will come about through better automated identification of bias (and other) errors and better techniques for determining boundary values. These improvements coupled with appropriate adjustments and improved data management techniques (e.g., Brown and Nelson, 1982) will allow the computation of more accurate vertical velocities over larger storm volumes than have previously been obtained.

7. ACKNOWLEDGMENTS

The authors are indebted to Messrs. C. Clark, R. Goldsmith and Ms. J. Kimpel for graphics used in the article. Ms. S. Mudd was responsible for typing of the manuscript.

This work was partially supported by National Science Foundation Grants ATM #74-03406a02 and ATM #781241 while the lead author was a graduate student at the University of Oklahoma.

8. REFERENCES

Armijo, L., 1969: A theory for the determination of wind and precipitation velocities with Doppler radars. J. Atmos. Sci., 26 (3), 570-573.

Bohne, A. R., and R. C. Srivastava, 1975: Random errors in wind and precipitation fall speed measurement by a triple Doppler radar system. Lab. for Atmospheric Probing Tech. Rept. No. 37, Univ. of Chicago-Illinois Institute of Technology, Chicago, Ill., 44 pp.

Brandes, E. A., 1977: Flow in severe thunderstorms observed by dual-Doppler radar. Mon. Wea. Rev., 105, 113-120.

Brown, R. A., and R. L. Peace, Jr., 1968: Mesoanalysis of convective storms utilizing observations from two Doppler radars. Preprints, 13th Conf. Radar Meteorology, Montreal, Amer. Meteor. Soc., Boston, 188-191.

_____ and S. P. Nelson, 1982: Multiple Doppler radar derived vertical velocities in thunderstorms: Part II - Maximizing areal extent of vertical velocities. NOAA Tech. Memo. ERL-NSSL-94, National Severe Storms Lab., Norman, Okla., 11-21.

_____, D. W. Burgess, J. K. Carter, L. R. Lemon, and D. Sirmans, 1975: NSSL dual Doppler radar measurements in tornadic storms: A preview. Bull. Amer. Meteor. Soc., 56 (5), 524-526.

Burgess, D. W., R. A. Brown, L. R. Lemon, and C. R. Safford, 1977: Evolution of a tornadic thunderstorm. Preprints, 10th Conf. Severe Local Storms, Omaha, Amer. Meteor. Soc., Boston, 84-89.

Carbone, R. E., 1981: Selected comments on multiple-Doppler analysis. Preprints, 20th Conf. Radar Meteorology, Amer. Meteor. Soc., Boston, 490-494.

Clark, T. L., F. I. Harris and C. G. Mohr, 1980: Errors in wind fields derived from multiple-Doppler radars: Random errors and temporal errors associated with advection and evolution. J. Appl. Meteor., 19, 1273-1284.

Doviak, R. J., P. S. Ray, R. G. Strauch, and L. J. Miller, 1976: Error estimation in wind fields from dual Doppler radar measurements. J. Appl. Meteor., 15 (8), 868-878.

Gal-Chen, T., 1978: A method for the initialization of the analastic equations: Implications for matching models with observations. Mon. Wea. Rev., 106 (5), 587-606.

_____, 1981: Estimation and correction of advection effects with single and multiple, conventional and Doppler radars. Preprints, 20th Conf. Radar Meteorology, Amer. Meteor. Soc., Boston, 606-612.

Hane, C. E., and B. C. Scott, 1978: Temperature and pressure perturbations within convective clouds derived from detailed air motion information: Preliminary testing. Mon. Wea. Rev., 106 (5), 654-661.

Heymsfield, G. M., 1978: Kinematic and dynamic aspects of the Harrah tornadic storm analyzed from dual-Doppler radar data. Mon. Wea. Rev., 106 (2), 233-254.

Kelly, T. J., H. W. Frank, G. B. Foote, and C. G. Wade, 1978: The Colorado hail-storm of 22 July 1976: II. Internal circulation. Preprints, 18th Conf. Radar Meteorology, Amer. Meteor. Soc., Boston, 219-225.

Lhermitte, R. M., 1970: Dual-Doppler radar observations of convective storm circulation. Preprints, 14th Conf. Radar Meteorology, Tucson, Amer. Meteor. Soc., Boston, 139-144.

Nelson, S. P., 1980: Hail production in a supercell storm using a Doppler derived wind field and a numerical hail growth model. NOAA Tech. Memo. ERL-NSSL-89, National Severe Storms Lab., Norman, Okla., 90 pp.

O'Brien, J. J., 1970: Alternate solutions to the classical vertical velocity problem. J. Appl. Meteor., 9, 197-203.

Ray, P. S., and K. K. Wagner, 1976: Multiple Doppler radar observations of storms. Geophys. Res. Letters, 3 (3), 189-191.

___, C. L. Ziegler, W. C. Bumgarner, and R. J. Serafin, 1980: Single- and multiple Doppler radar observations of tornadic storms. Mon. Wea. Rev., 108, 129-147.

MULTIPLE DOPPLER RADAR DERIVED VERTICAL VELOCITIES IN THUNDERSTORMS: PART II - MAXIMIZING AREAL EXTENT OF VERTICAL VELOCITIES

Rodger A. Brown and Stephan P. Nelson

Abstract

Vertical velocities are deduced from multiple Doppler radar measurements through vertical integration of the three-dimensional mass continuity equation. However, vertical velocity information is lost in those vertical columns that do not have a continuity of Doppler radar data. This situation becomes critical in studies of the more severe thunderstorms where the very updrafts that the researcher is attempting to study are the cause of data gaps (e.g., weak echo regions). Problems also arise when multiple Doppler radar data are not collected to storm top. This paper explores some techniques that can be used to extract the greatest amount of vertical velocity information from these problem data sets.

1. INTRODUCTION

With the advent of dual Doppler radar measurements in convective storms in 1967 (Brown and Peace, 1968; Browning et al., 1968) came the opportunity to determine the kinematic properties of storms and to deduce the associated microphysical, dynamical and thermodynamical characteristics. As part of this effort, the computation of realistic vertical velocity values throughout storm depth has been a continuing challenge.

Since vertical velocities are obtained through vertical integration of the mass continuity equation, small errors in the boundary value or in the divergence field (computed from horizontal winds) produce vertical velocity errors that amplify with upward integration. Thus most of the early investigators limited their discussions to the lower portions of storms (e.g., Lhermitte, 1970; Brown et al., 1975; Brandes, 1977; Burgess et al., 1977; Heymsfield, 1978). Studies showing data throughout storm depth typically displayed updrafts and downdrafts whose magnitudes tended to increase with height (e.g., Kropfli and Miller, 1975; Miller, 1975).

Bohne and Srivastava (1975) showed that there is a distinct advantage to integrating from storm top to the ground, as opposed to the more conventional upward direction, when vertical velocity is constrained to be zero only at the initial boundary. The decrease of air density with upward integration acts to amplify both initial boundary value errors and accumulated divergence errors. On the other hand, the increase of density from storm top toward the ground not only damps divergence errors but actually decreases the contribution of initial boundary value errors. Therefore, except when data of interest are near the ground, downward integration produces much more realistic vertical velocity profiles than does upward integration.

However, a major problem still remained to be addressed--namely, the point that vertical velocity (w) should be zero at both the ground and storm top. O'Brien (1970) provided a solution to this problem as part of his work with rawinsonde data. In general terms, the procedure is to set w equal to zero at one boundary and integrate horizontal divergence upward or downward to obtain a nonzero w value at the final boundary. Assuming that w should be zero at the final boundary, the computed value there represents accumulated w error due to small horizontal wind errors. Taking the vertical distribution of air density into account, a w correction factor can be computed for each vertical integration step by assuming that the error is the same for all steps. The corrected vertical velocity profile then has zero velocity for both the bottom and top boundary values. Approaches along this line have been applied successfully to multiple Doppler radar studies during the past few years (e.g., Miller, 1980; Nelson, 1980; Ray et al., 1980; Brown et al., 1981; Nelson and Brown, 1982).

With the conceptual vertical velocity problems solved, there remain a few practical problems. One problem is: What do we do when multiple Doppler data do not extend all the way to storm top? Considering how infrequently severe storms pass through a multiple Doppler radar network, it would be unfortunate to lose vertical velocity information throughout a storm because only one radar collected data to storm top. Another question is: What do we do when there are data gaps in a vertical column that prevent us from computing w in that column? The purpose of this paper is to provide some practical solutions to these problems.

2. MULTIPLE DOPPLER RADAR METHODOLOGY

Before exploring the missing data problem, it is desirable to understand the synthesis procedures for two and for three or more Doppler radars. The synthesis process provides an estimate of the mean three-dimensional velocity of precipitation particles in the radar sampling volume. Particle velocity is defined by the three components of air motion (u,v,w)--assuming that precipitation is a faithful tracer of air motion--and the mean terminal fall velocity in still air (V_t). The objective is to solve for these four unknowns.

2.1 Two Doppler Radars

A general dual Doppler synthesis procedure was presented by Armijo (1969). A modified technique that solves for the velocity components directly on a cartesian grid was developed jointly by Brandes (1977) and Brown et al. (1981). With four unknowns and two equations (one Doppler velocity measurement from each radar), two other equations are used: the equation for three-dimensional mass continuity of air and an empirical relationship between V_t and the measured radar reflectivity factor. The resulting air motion components are:

$$u = A + (w + V_t)B \tag{1}$$

$$v = C + (w + V_t)D \tag{2}$$

$$w_n = w_b - \int_b^n \left(\frac{w}{\rho}\frac{\partial \rho}{\partial z} + \frac{\partial u}{\partial x} + \frac{\partial v}{\partial y}\right) dz \qquad (3)$$

where A, B, C and D are functions of the measured Doppler velocities and the three-dimensional radar geometry and ρ is air density. The uncorrected vertical velocity at height n (w_n) is a function of w_b at the initial boundary height and the integrated contribution of density and horizontal divergence ($\partial u/\partial x + \partial v/\partial y$) from the initial boundary to height n.

Note that u, v and w are interrelated. A procedure is to iterate the computation of u, v and w at each level until the w change becomes less than a specified value (such as 0.01 m s^{-1}), then to repeat the process at each successive level.

The fact that all three velocity components are interrelated means that if all three can not be determined then none of them can be determined. More importantly, if at least one of the three components is missing at any height, u, v and w values can not be computed in the entire column. Therefore, it is imperative for the synthesis of dual Doppler data to have techniques for handling data gaps.

2.2 Three or More Doppler Radars

Armijo (1969) also outlined a typical procedure for synthesizing measurements from three or more Doppler radars into the three components of precipitation motion:

$$u = E \qquad (4)$$

$$v = F \qquad (5)$$

$$(w + V_t) = G \qquad (6)$$

where E, F and G are functions of the measured Doppler velocities and the three-dimensional radar geometry. In this situation, precipitation motion is uniquely specified at each grid point where data from all radars exist, regardless of vertical data continuity. However, the vertical component of air motion (w) is not uniquely specified.

Armijo proposed that an equation of continuity for V_t be used in conjunction with Eq. (6) to separate w and V_t. However, from a practical viewpoint, the quantity G turns out to have an unrealistically large value when the storm of interest is not near the center of the area encompassed by the Doppler radars; that is, problems arise when one of the radars has such a low elevation angle that it does not adequately measure the vertical component of motion (e.g., Miller, 1980; Nelson, 1980).

In practice, w may be computed from Eqs. (3)-(5), where the mass continuity equation has been employed. Even though u and v are determined at all grid points having radar data, computation of corrected w values at all grid points in a vertical column is prevented by the presence of data voids in the integration column. Thus, even with three or more Doppler radars, data gaps present problems that deserve careful consideration.

3. TECHNIQUES FOR HANDLING DATA VOIDS

Fortunately there are effective techniques for estimating vertical velocities in portions of storms where data do not exist from the ground through storm top. (Storm top typically is specified by the minimum radar reflectivity factor that is associated with usable Doppler velocity data.) In the following discussion downward integration is assumed; in fact, some of the techniques are not possible with upward integration.

Figure 1 shows a hypothetical radar echo outline of a supercell severe thunderstorm including various storm areas that benefit from these techniques. This storm outline illustrates an extreme situation that is a source of great frustration for those who attempt to synthesize a three-dimensional flow field from multiple Doppler radar data. Using conventional synthesis approaches, corrected w values could be computed only in the areas labeled A. By applying the techniques presented here (and their associated assumptions) the area where corrected vertical velocities can be computed expands into all unshaded regions.

3.1 Technique A - Data From Ground to Storm Top

Under ideal conditions (three or more Doppler radars, storm near center of multiple Doppler area, realistic estimate of V_t), w at the top boundary can be estimated from Eq. (6) as follows (e.g., Armijo, 1969; Bohne and Srivastava, 1975):

$$w = G - V_t$$

However, in the more typical situation (storm not at center of multiple Doppler area, only two Doppler radars available), the best one can do is to make a reasonable estimate for the boundary value, such as zero vertical velocity. The magnitude of w errors likely to be encountered in the constrained vertical velocity field due to erroneous boundary values is discussed by Nelson (1980) and Nelson and Brown (1982).

A related concern is whether w can be assumed equal to zero along the entire sloping echo top (as shown in Fig. 1). One can argue that the highest portion of the radar echo is the top of the main updraft and that the sloping surface represents horizontally diverging air. With this interpretation, the assumption of a zero w boundary condition along the entire top surface seems reasonable.

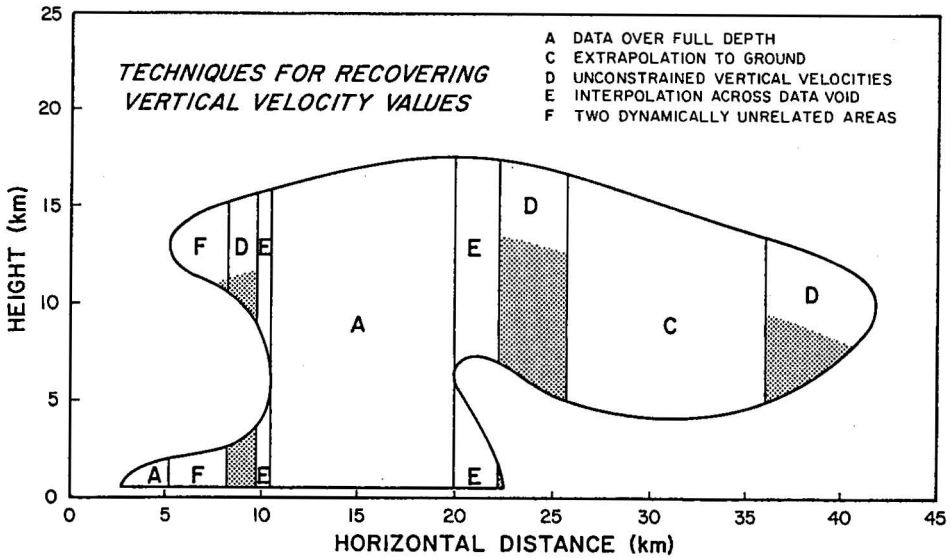

Figure 1. Overview of portions of a supercell storm where various techniques can be used to recover vertical velocity values where they otherwise would not be computed. Realistic vertical velocities cannot be estimated in the shaded areas.

A question then may arise concerning the upper boundary value when the radar echo top in a particular vertical column is much lower than the main storm top--such as the area labeled A in the lower left portion of Fig. 1. In this region of low-level convection, w could be set equal to zero if the area were not growing vertically; if it were growing, then the rate of echo rise could be used to estimate the w boundary value. If there is no interest in low-level convection, an echo top threshold height can be defined, such that all w values are set equal to missing for data columns that do not extend above that height. A threshold height set anywhere between 3 and 10 km in Fig. 1 would set low-level area A (and F, as discussed later) equal to missing while initializing w along the entire top surface of the radar echo.

A second place where an assumption has to be made is just above the ground. Since a storm always is some distance from at least one radar, the drop-off due to earth's curvature puts the lowest common data level at least a few tenths of a kilometer above the earth's surface. In order to establish the lower boundary condition of w=0 at the ground, an estimate for the divergence between the lowest grid level and the ground must be made. The severe storm vertical velocity profiles and associated divergence profiles in Figs. 2 and 3 suggest that one would not be significantly in error by assuming that divergence is constant from the lowest grid level to the ground. Since air is a fluid with three-dimensional continuity, there should be no marked divergence discontinuities over depths of 1 km or less.

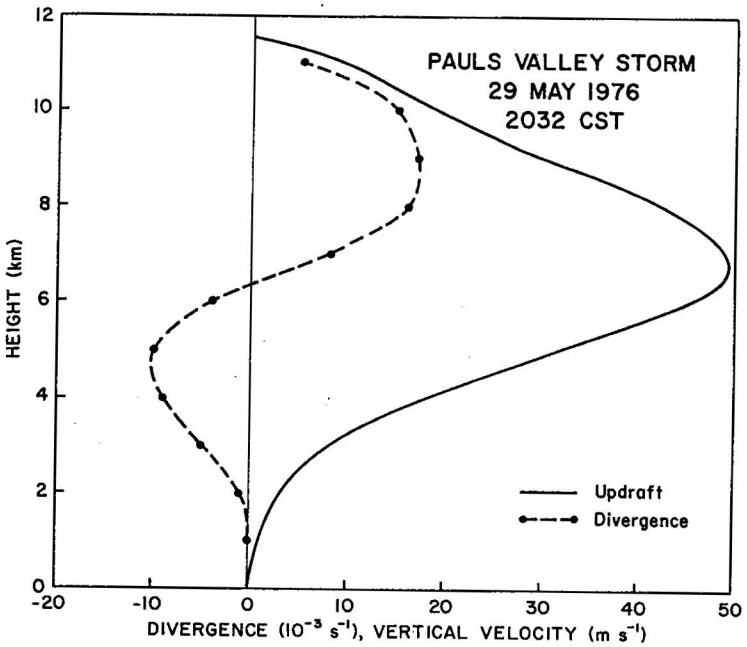

Figure 2. Updraft profile (constrained to zero at ground and at one-half grid interval above top data level) and associated divergence profile derived from triple Doppler radar data.

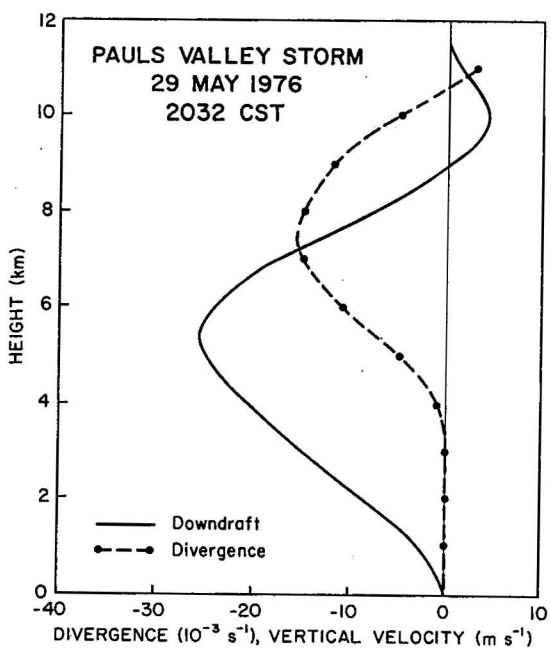

Figure 3. Downdraft profile (constrained to zero at ground and at one-half grid interval above top data level) and associated divergence profile derived from triple Doppler radar data.

3.2 Technique B - Data Missing in Upper Portion of Storm

Since multiple Doppler radar data usually are collected at successive constant elevation scans from the ground upward, there are times when one of the radars ceases data collection before storm top is reached. When at least two radars have data at storm top, it is possible to include these fewer radars in the synthesis process. However, when the highest multiple Doppler data level is below storm top, some assumptions must be made. Assuming that w is zero at the highest data level might be acceptable in most storm regions, but it is not acceptable within the main updrafts and downdrafts.

Nelson (1980) has developed a technique for initializing w at the highest data level, provided that it is well above the level of maximum vertical velocity. The gist of the technique is to initially assume that w is zero at the top grid level (and at the ground) and to integrate downward to find the locations of the major updrafts and downdrafts (for an example, see curve A in Fig. 4). Based on the height of storm top and the vertical profile of velocity at the core of each significant updraft, a first guess can be used to reinitialize the core updraft value at the top grid level. In Fig. 4, an extrapolation of curve B (reinitialized at 30 m s^{-1}) falls short of the observed storm top; the extrapolation procedure maintains the data trend. A reasonable second guess would be 40 m s^{-1}, but 60 m s^{-1} (curve C) was chosen for this example to show how quickly the initial boundary error is damped with decreasing height; after a descent of only 3 km, the overall velocity difference has decreased from 60 m s^{-1} to 20 m s^{-1}. Based on curves B and C, one can estimate that the initial core w value for this updraft should be about 35 m s^{-1}.

If multiple Doppler radar data were collected to storm top at adjacent time periods, another technique can be used. The updraft and downdraft values at the

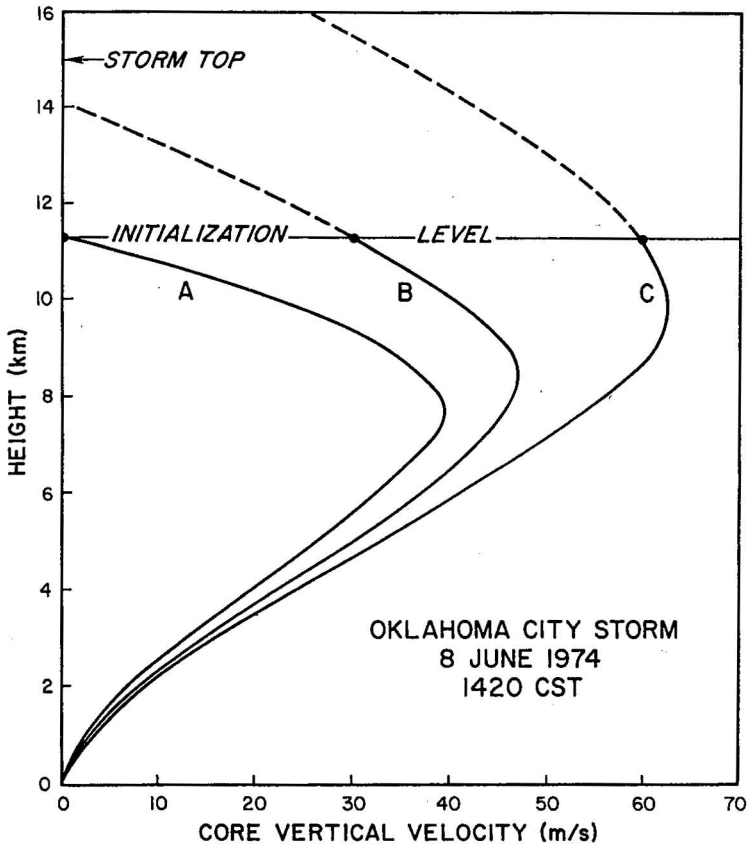

Figure 4. Vertical velocity curves initialized at top data level (below storm top) using values of 0 (A), 30 (B), and 60 m s^{-1} (C). Dashed curves are extrapolated. Example of Technique B applied to dual Doppler radar data.

top data level can be estimated from interpolated (or extrapolated) w values from adjacent times at the same height.

3.3 Technique C - Data Missing at Lower Storm Levels

When data are missing--due to either absence of data collection or lack of radar echo--in the lower portions of a storm, it still is possible to compute w in at least part of the vertical data column. If the lowest data level is sufficiently close to the ground, the divergence value (or divergence gradient) at that level can be extrapolated to the ground, making it possible to compute adjusted w values at the levels with data.

There is a question of how far the divergence values realistically can be extrapolated. Figures 5 and 6 show two divergence profiles and their corresponding vertical velocity profiles for extrapolation distances of 0.5, 2.5, 4.5 and 6.5 km. In each case, divergence was assumed to be constant from the lowest data level (black square) to the ground. The two figures illustrate the sensitivity of the w curve to the divergence value at the lowest data level relative to the divergence profile below that level. Since the extrapolated divergence values in Fig. 5 are not good approximations of the divergence profile, the partial w curves differ from the "true" curve (lowest data level at 0.5 km) by over 10 m s^{-1} at all heights below 9 km. By contrast, the divergence curve in Fig. 6 is uniform below 6.5 km, so the partial w curves are very good approximations to the "true" curve.

In reality, divergence below the lowest data level is not known. Therefore, caution is advised when applying Technique C. Perhaps some confidence can be gained by looking at the trend of the portion of the divergence profile that does

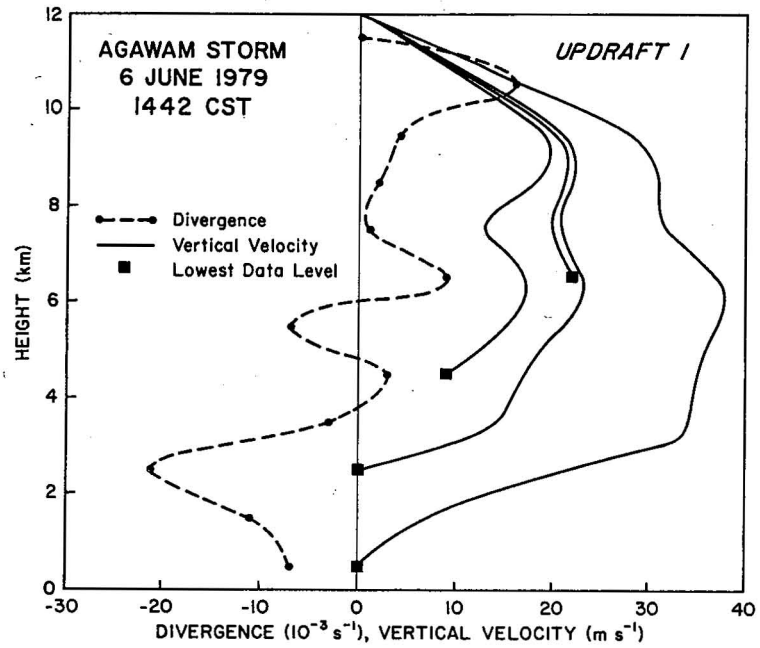

Figure 5. Divergence profile and associated updraft profiles computed by assuming divergence to be constant from the lowest data levels (square at 0.5, 2.5, 4.5, and 6.5 km) to the ground. Example of Technique C applied to dual Doppler radar data.

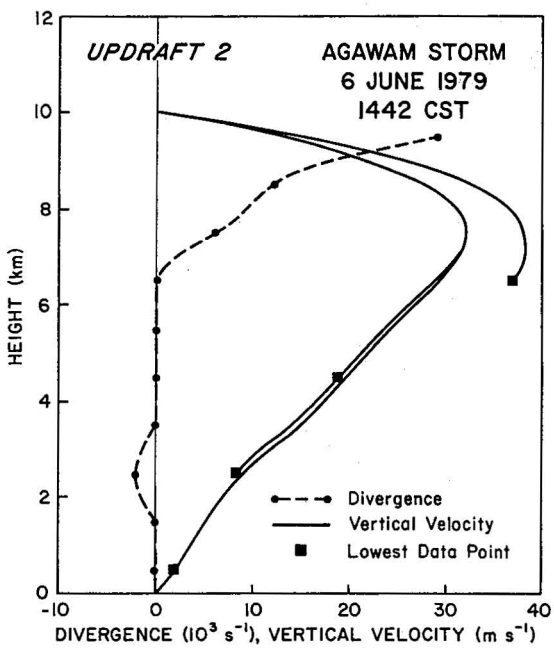

Figure 6. Same as Fig. 5 for a different updraft.

exist. The area labeled C in Fig. 1 indicates where adjusted vertical velocities can be computed when divergence is extrapolated over a depth of 5 km.

3.4 Technique D - Data Missing in Lower and Middle Portions of Storm

If the lowest data level is too far above the ground to extrapolate divergence, it is not possible to constrain the vertical velocity profile and thereby eliminate accumulated errors. Therefore, in order to compute any w values in a vertical column, one must be willing to accept some uncertainty in the values.

Typical errors associated with unconstrained (that is, unadjusted) vertical velocities for downward integration are shown in Fig. 7; the errors represent differences between constrained and unconstrained w values for updrafts and downdrafts that extended from storm top (or top data level) to the ground. After 3 to 5 integration steps (at 1 km interval), most accumulated errors have grown to about 10 m s^{-1}. With an actual data set one can determine what the number of unconstrained integration steps should be by comparing the unconstrained w values with surrounding constrained values.

The regions labeled D in Fig. 1 are where Technique D has been applied over four integration steps of 1 km. The shaded area in the remainder of each column reflects excessive accumulated w errors.

3.5 Technique E - Data Gaps Within the Storm

At times there are breaks in a vertical data column where data are missing for several different reasons (e.g., no data collected, weak reflectivity due to irregular echo boundaries). Using the conventional synthesis procedure, w could not be computed in that column. However, if that gap is in the bounded weak echo region of a severe storm--where the storm's main updraft is located--knowledge of w in that and adjacent columns is greatly desired for an understanding of storm dynamics.

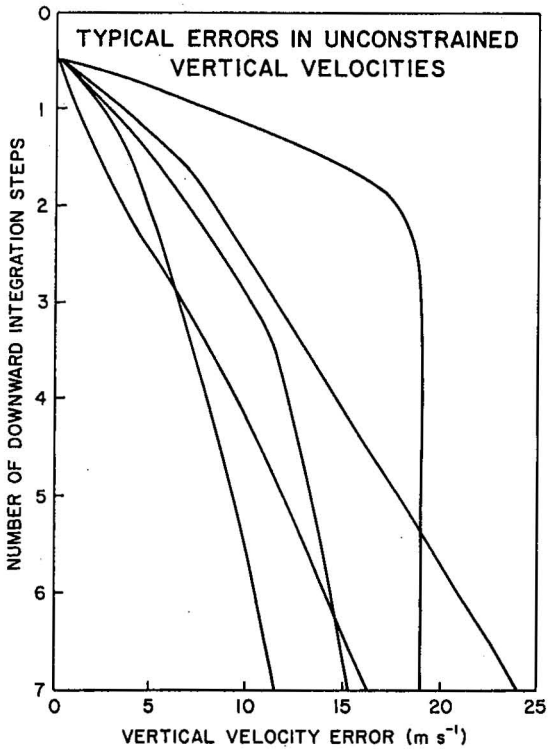

Figure 7. Vertical velocity errors contained in unconstrained updraft and downdraft profiles from the Oklahoma City (8 June 1974) and Agawam (6 June 1979) storms. Errors represent the difference between constrained and unconstrained core vertical velocity profiles (top boundary value assumed to be zero at one-half grid interval above top data level). Downward integration was performed in 1 km steps.

Technique E uses the average of the divergence values at the top and bottom of the gap to continue w computations below the gap. From the divergence profiles in Figs. 2 through 6, it appears that the average divergence over a depth of several kilometers does not drastically affect the vertical velocity profiles. For the hypothetical areas labeled E in Fig. 1, divergence is interpolated over depths of up to 5 km in order to estimate w throughout the column.

3.6 Technique F - Data Voids Between Dynamically Unrelated Data Regions

With the more energetic severe thunderstorms, it is possible to have low level convection in the flanking line associated with the gust front and to have an upwind anvil overhang at high levels. Since the two storm regions are not dynamically connected in the same vertical column, it is appropriate to initialize w at the top of both regions. Data inspection permits one to determine the depth of the data void (greater than or equal to that used for Technique E) that must be exceeded before w at the top of the lower data region is reinitialized; the critical depth shown in Fig. 1 is 8 km.

Since corrected w values can not be computed for the upper data region (F), vertical velocities are handled as with Technique D. The lower data region contains corrected w values when the top of each data column in the region is above the threshold height used in Technique A.

4. SUMMARY

Since few convective storms have flat tops and vertical edges with data existing throughout the entire depth from the ground to storm top, various assumptions must be made to compute vertical velocities where multiple Doppler radar measurements are available. The more severe the storm, the more likely that radar features such as echo overhangs and bounded weak echo regions prevent the straightforward computation of w, and of u and v in the case of dual Doppler data.

In this paper we have discussed several techniques that can be used to estimate w in regions of a storm where vertical velocities otherwise could not be computed. These techniques have proven to be very valuable in optimizing the recovery of vertical velocity information in a variety of severe thunderstorms.

5. ACKNOWLEDGMENTS

This study has been supported in part by the Department of Energy, Federal Aviation Administration and Nuclear Regulatory Commission. We appreciate Sandra Mudd's careful typing of the manuscript and Joan Kimpel's expert figure preparation.

6. REFERENCES

Armijo, L., 1969: A theory for the determination of wind and precipitation velocities with Doppler radars. J. Atmos. Sci., 26, 570-573.

Bohne, A. R., and R. C. Srivastava, 1975: Random errors in wind and precipitation fall speed measurement by a triple Doppler radar system. Tech. Rep. No. 37, Lab. for Atmos. Probing, Univ. of Chicago, 44 pp.

Brandes, E. A., 1977: Flow in severe thunderstorms observed by dual-Doppler radar. Mon. Wea. Rev., 105, 113-120.

Brown, R. A., and R. L. Peace, Jr., 1968: Mesoanalysis of convective storms utilizing observations from two Doppler radars. Preprints, 13th Conf. Radar Meteorology, Amer. Meteor. Soc., Boston, 188-191.

_____, D. W. Burgess, J. K. Carter, L. R. Lemon and D. Sirmans, 1975: NSSL dual-Doppler radar measurements in tornadic storms: A review. Bull. Amer. Meteor. Soc., 56, 524-526.

_____, C. R. Safford, S. P. Nelson, D. W. Burgess, W. C. Bumgarner, M. L. Weible, and L. C. Fortner, 1981: Multiple Doppler radar analysis of severe thunderstorms: Designing a general analysis system. NOAA Tech. Memo. ERL NSSL-92, National Severe Storms Lab., Norman, Okla., 21 pp.

Browning, K. A., T. W. Harrold, A. J. Whyman and J. G. D. Beimers, 1968: Horizontal and vertical air motion, and precipitation growth, within a shower. Preprints, 13th Conf. Radar Meteorology, Amer. Meteor. Soc., Boston, 122-127.

Burgess, D. W., R. A. Brown, L. R. Lemon and C. R. Safford, 1977: Evolution of a tornadic thunderstorm. Preprints, 10th Conf. on Severe Local Storms, Amer. Meteor. Soc., Boston, 84-89.

Heymsfield, G. M., 1978: Kinematic and dynamic aspects of the Harrah tornadic storm analyzed from dual-Doppler radar data. Mon. Wea. Rev., 106, 233-254.

Kropfli, R. A., and L. J. Miller, 1975: Thunderstorm flow patterns in three dimensions. Mon. Wea. Rev., 103, 70-71.

Lhermitte, R. M., 1970: Dual-Doppler radar observations of convective storm circulation. Preprints, 14th Conf. Radar Meteorology, Amer. Meteor. Soc., Boston, 139-144.

Miller, L. J., 1975: Internal airflow of a convective storm from dual-Doppler radar measurements. Pageoph, 113, 765-785.

_____, 1980: Dynamical-microphysical evolution of a convective storm: Part II - Airflow from multiple Doppler radar observations. NCAR Tech. Note TN-151+STR, Natl. Center for Atmos. Res., Boulder, 69-120.

Nelson, S. P., 1980: A study of hail production in a supercell storm using a Doppler derived wind field and a numerical hail growth model. NOAA Tech. Memo. ERL NSSL-89, National Severe Storms Lab., Norman, Okla., 90 pp.

_____ and R. A. Brown, 1982: Multiple Doppler radar derived vertical velocities in thunderstorms: Part I - Error analysis and solution techniques. NOAA Tech. Memo. ERL-NSSL-94, National Severe Storms Lab., Norman, Okla., 1-10.

O'Brien, J. J., 1970: Alternative solutions to the classical vertical velocity problem. J. Appl. Meteor., 9, 197-203.

Ray, P. S., C. L. Ziegler, W. C. Bumgarner and R. J. Serafin, 1980: Single- and multiple-Doppler radar observations of tornadic storms. Mon. Wea. Rev., 108, 1607-1625.